

PAPER • OPEN ACCESS

## Preliminary tests on additive-manufactured Al-Sc specimens for the setup of a numerical model for Laser Shock Peening

To cite this article: Nicola Zavatta and Enrico Troiani 2023 *J. Phys.: Conf. Ser.* **2526** 012044

View the [article online](#) for updates and enhancements.

### You may also like

- [Effects of overlap rate and energy density on mechanical properties of Inconel 718 by multiple small-spot-LSP impacts](#)  
Woyun Lv, Zhanqiang Liu, Yang Hua et al.
- [Laser shock peening and its effects on microstructure and properties of additively manufactured metal alloys: a review](#)  
Michael Munther, Tyler Martin, Ali Tajyar et al.
- [Microstructure and mechanical properties of Be-Al and Be-Al-Sc alloys with various solidification rates](#)  
Liangbo Yu, Jing Wang, Xiandong Meng et al.

# Preliminary tests on additive-manufactured Al-Sc specimens for the setup of a numerical model for Laser Shock Peening

Nicola Zavatta and Enrico Troiani

Department of Industrial Engineering - DIN, University of Bologna, 47121, Forlì, Italy

E-mail: nicola.zavatta2@unibo.it, enrico.troiani@unibo.it

**Abstract.** Aluminum-Scandium alloys offer a great potential in aerospace applications due their high corrosion resistance and improved strength properties. Furthermore, these alloys have been qualified for laser additive manufacturing (AM), producing parts with static strengths rivalling their conventionally manufactured counterparts. However, laser processing also results in large residual stresses that can severely affect fatigue properties and result in geometric distortion. A proven method for reducing the fatigue-related problems in metallic structures is to drive compressive residual stresses into the affected area by means of Laser Shock Peening (LSP). This surface treatment is very effective in bulk structures, improving life performances of fatigue-sensitive aeronautical components, such as jet engines turbine blades or helicopter gearboxes. On the other hand, quite a limited number of studies has been presented on the effect of LSP on fatigue crack growth in thin components and laser AM structures. This work presents first the results of preliminary tensile tests on additive manufactured Al-Sc specimens. The tensile strengths of as-built and heat-treated samples are compared. Then, a reliable and computationally time-effective numerical model of laser peening is reviewed, referring to case studies investigated earlier. In view of applying LSP to additive manufactured Al-Sc components, the effects of different laser parameters and geometries are discussed. Finally, the possible drawbacks of the LSP treatment are addressed, in order to exploit its full potential in increasing the fatigue life of AM components.

## 1. Introduction

The continuous quest for reduced emissions and increasing efficiency is driving the research of lightweight materials in the aerospace field. While the use of composites has increased substantially, innovative lightweight alloys such as Aluminum-Scandium are also very promising, particularly when combined with Additive Manufacturing (AM). With its unique ability to produce complex structures, while reducing the assembly cost and optimizing the material efficiency, additive manufacturing is of extreme interest for the aerospace industry [1]. Various Al-Sc powders have been qualified for laser additive manufacturing, offering properties equal to or even better than their conventionally manufactured counterparts. However, the fatigue resistance of additive-manufactured components is impaired by the residual stresses induced during manufacturing.

A proven technique to improve the fatigue properties of metallic parts is Laser Shock Peening (LSP). It is a surface treatment in which high-power laser pulses are shot at the metal surface. The laser beam vaporizes a superficial layer of the material or a specific coating (e.g. a thin



layer of pure aluminum), with the formation of a high-pressure plasma, which is confined by a transparent overlay (usually water). Following evaporative breakdown of the overlay, the plasma expands rapidly, generating compressive shock waves that propagate in the material and induce compressive residual stresses. Laser peening has already found application in aeronautics, in components such as engine turbine blades, wing attachment lugs and helicopter gearboxes, and is very effective in this kind of bulk structures [2].

The effectiveness of LSP in improving the fatigue properties of aluminum alloys is well documented in the literature [3, 4]. In particular, Gao [4] observed laser peening is superior to mechanical shot peening in enhancing the fatigue performance, thanks to deeper compressive stresses and better surface finish. However, limited studies have been presented on the fatigue crack growth in thin light alloys components [5] where, as a consequence of the self-balancing residual stress field induced by the LSP in the thin-gauge panel, the chosen peening pattern configuration (distance of the crack tip to the laser shot, width of the laser pattern) can affect significantly the fatigue crack propagation performances [6, 7].

Most investigations have dealt with the physical aspects of LSP, focusing attention on the optimized setups for best residual stress distribution and, hence, performances of the treated metallic material. In this regard, several experimental studies have been carried out to investigate the role of laser parameters and, at the same time, optimize the process. However, sophisticated techniques are needed for the measurement of residual stresses, such as X-Ray Diffraction (XRD) and Incremental Hole Drilling (IHD). Furthermore, the high strain rates involved (about  $10^6$  1/s), combined with the transient nature of LSP, make real-time monitoring of the process very challenging. For these reasons, reliable simulation techniques are used in achieving a good knowledge of LSP applications and phenomena, allowing time and cost reductions [8].

The aim of our work is to apply laser shock peening to additive-manufactured Al-Sc alloy to improve its fatigue properties. In this article, we present a preliminary assessment of the quasi-static mechanical properties of Al-Sc specimens. Moreover, we discuss a numerical model to compute the residual stresses induced by LSP, which has previously been developed, and review its applications to real case studies.

## 2. Materials and methods

Preliminary tests were conducted on additive manufactured Al-Sc specimens. In particular, the ultimate tensile strength (UTS) and surface hardness of the specimens were measured to assess the mechanical properties of the alloy in anticipation of further testing. In the following section, the details of the experiments are given. Moreover, the numerical model for the simulation of laser shock peening is presented.

### 2.1. Experimental setup

The tensile tests were performed on flat dog-bone specimens made of Scalmalloy. Scalmalloy<sup>®</sup> (produced by Carpenter Additive<sup>®</sup>) is an Aluminum-Scandium powder specifically designed for additive manufacturing applications and provides high static strength even when compared to aluminum alloys manufactured by conventional techniques. The nominal composition of Scalmalloy powder is reported in table 1.

The specimens were produced by Laser Powder Bed Fusion (L-PBF) in a single batch. They were then divided in two groups: the first was tested in the as-built condition (AB), while the second was subjected to heat treatment at 325°C for 4 hours before testing (HT). The temperature and duration of the heat treatment were selected according to the material datasheet. In total, three specimens for each group were tested.

The tensile tests were carried out under displacement control in quasi-static loading conditions. The ultimate tensile strength was recorded by the test bench, while the strain

**Table 1.** Nominal chemical composition of Scalmalloy<sup>®</sup> powder.

Al	Mg	Sc	Mn	Zr	Fe	Si	Others
Balance	4.20-5.10 %	0.60-0.88 %	0.30-0.80 %	0.20-0.50 %	0.40 %	0.40 %	0.65 %

was measured using an extensometer. The test set-up is shown in figure 1. In addition to the tensile tests, the surface hardness was also measured. Since the specimens had not been machined after manufacturing and their surface roughness was considerable, the measurement areas were polished prior to hardness testing. The tests were performed according to Brinell HB/30 method.

**Figure 1.** Tensile tests setup.

## 2.2. Numerical model

The residual stresses induced by laser shock peening can be estimated by means of numerical simulations. A finite element model to simulate LSP has been developed and validated in earlier works [9, 10, 11]. In this model, the interaction between the laser beam and metal surface and the process of plasma formation are not directly simulated. Instead, the pressure profile resulting from plasma expansion is applied as a load acting on the metal surface, following an approach similar to that of Peyre et al. [12].

One simulation consists of applying the surface pressure and computing the propagation of pressure waves across the specimen and subsequent material relaxation. Hence, the simulation is divided in two steps: first, an equivalent pressure profile is applied in the peened area, generating elastic waves in the material; second, the constraints are released and residual stresses arise, following material relaxation. The applied pressure profile is shown in figure 2. Its shape reflects that observed in experimental measurements, with a pressure peak followed by a steady decrease due to elastic release. The magnitude of the pressure peak is related to laser intensity

and wavelength. For instance, for a laser with 1064 nm wavelength and 4 GW/cm<sup>2</sup>, the peak pressure is approximately 3.5 GPa. Each simulation can be repeated by iterating the application of pressure, so to simulate overlapping laser peens. This yields a more accurate prediction of residual stresses, though at the cost of increased computational time.

The model has been implemented in Abaqus software. An hexahedral mesh is used to discretize the structure, with a refined mesh size around the peened area (as shown in figure 2). Because of the large deformations involved, an explicit method is used to solve the finite element equations. The material model needs to account for plastic flow at very high strains and strain rates. Two alternative formulations can be used: Johnson-Cook (JC) plasticity model and kinematic hardening (KH) plasticity model.

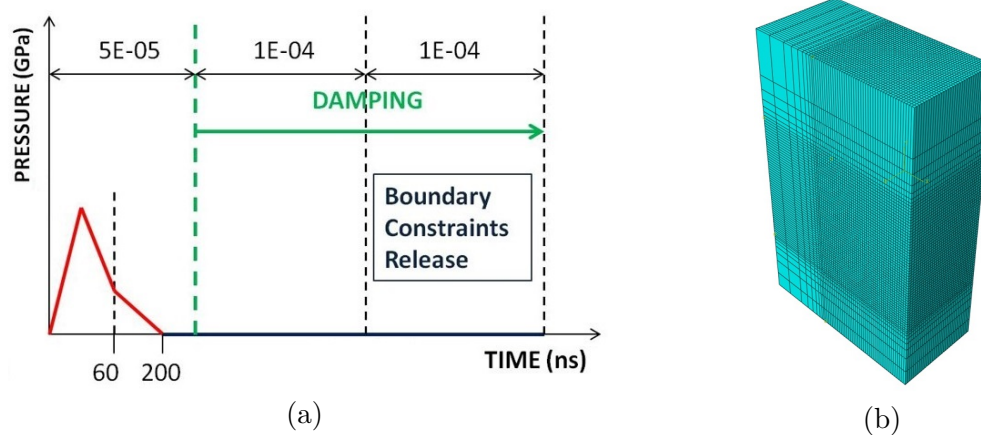


**Figure 2.** Numerical model: (a) pressure profile applied in the simulations, (b) example of mesh refinement around the peened area.

Johnson-Cook model [13] describes the flow stress as a product of three terms: strain hardening, strain rate and temperature. In our model, the effect of temperature on plastic flow is neglected, so that JC formulation becomes:

$$\sigma_Y = (A + B\varepsilon^n)(1 + C \ln(\frac{\dot{\varepsilon}}{\dot{\varepsilon}_0}))$$

where  $A$  is the yield strength (at room temperature),  $B$  and  $n$  are the strain hardening coefficients, and  $C$  is the strain rate coefficient.

The kinematic hardening model is based on a work by Chaboche [14]. The plastic flow is modelled as a combination of isotropic hardening and nonlinear kinematic hardening, according to the following equations:

$$\begin{aligned} \sigma_Y &= \sigma_0 + Q_\infty(1 - \exp(-b\varepsilon^{pl})) \\ \dot{\alpha} &= C\varepsilon^{pl} - \gamma\alpha|\dot{\varepsilon}^{pl}|. \end{aligned}$$

Here,  $\alpha$  denotes the kinematic hardening component (backstress),  $\sigma_0$  is the initial yield strength,  $Q_\infty$  and  $b$  are the isotropic hardening coefficient and exponent, and  $C$  and  $\gamma$  are the kinematic hardening modulus and rate, respectively. The model parameters need to be measured by experimental tests, see for instance [15].

### 3. Results and discussion

In the following, the results of the tensile tests and hardness measurements are first shown. Then, examples of application of the numerical model to real case studies from previous works are reviewed and discussed.

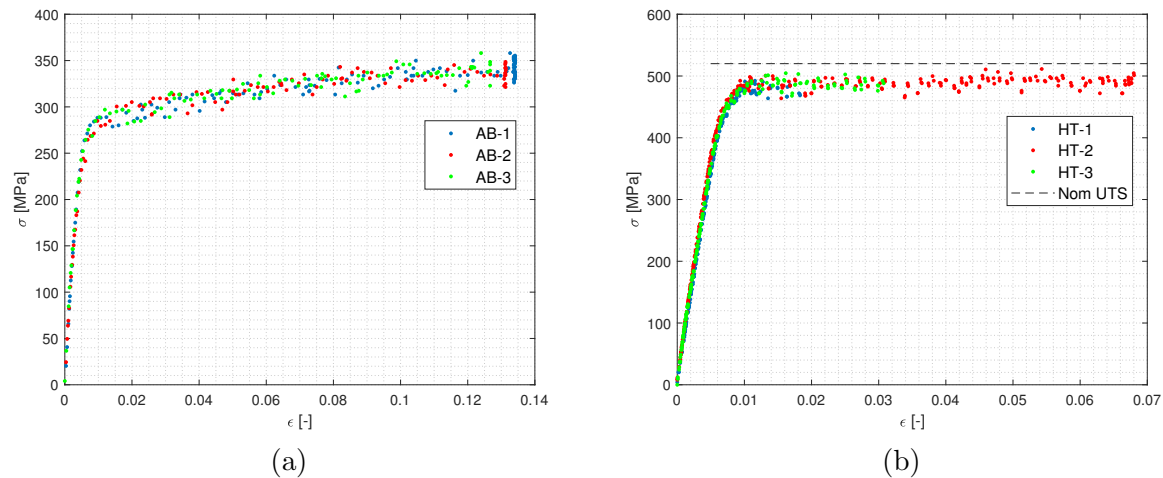


**Figure 3.** Stress-strain curves measured in tensile tests: (a) as-built samples, (b) heat-treated samples. The nominal UTS for the heat-treated condition is also reported as a dashed line.

### 3.1. Mechanical tests

The stress-strain curves measured in the tensile tests are reported in figure 3. For both the as-built and the heat-treated samples, data within the same group are self-consistent, i.e. deviations between specimens belonging to the same group are limited. In particular, the ultimate tensile strengths of specimens within each of the two groups differ by less than 5%. The average UTS of the untreated samples is about 350 MPa, while that of the heat-treated samples is about 490 MPa, approximately 6% lower than the nominal value reported for Scalmalloy, namely 510-530 MPa.

These values are in agreement with recent observations by Raab and Bambach [16], who reported strengths of approximately 510 MPa for Scalmalloy specimens treated at 325°C for 2 hours and 350 MPa for untreated samples. Similar strength increments following heat treatment were found by Spierings et al. [17], with an UTS of 520 MPa for treated samples (325°C for 4 hours) and 410 MPa in the as-built condition.

A large scatter is observed in the strain at failure of the heat-treated-samples, with values ranging from 1.8% to 6.8%. These values are remarkably lower than the nominal one of 13-16% reported in the datasheet. This contrasts with the behaviour observed in the as-built samples, whose ultimate strain exhibits only little scatter.

Previous works also reported a decrease of the failure strain in heat-treated samples, which was accompanied by an increase of the tensile strength [17, 16, 18]. Notably, Ren et al. [18] found a significant decrease of the ultimate strain in additive manufactured Al-Mg-Sc-Zr alloy subjected to heat treatment at 300°C for 4 hours. Following observations of SEM (Scanning Electron Microscopy) images of the fracture surface, the authors explained this effect as an increased size of cleavage surface and dimple density, which results in less plasticity. It is plausible that a similar mechanism occurs in the heat-treated Scalmalloy specimens, thus leading to the embrittlement observed in the tensile tests.

The average Brinell hardness was 101.1 HB30 for the as-built samples and 146.3 HB30 for the heat-treated ones. As a comparison, Spierings et al. [17] found an average surface hardness of about 135 HB for Scalmalloy specimens heat-treated at 325°C for 4 hours. That thermal treatment could substantially improve the surface hardness of Scalmalloy has also been recently reported by Raab and Bambach [16]. The authors observed an hardness increase from 99 HB2.5 to 156 HB2.5 by applying an ageing treatment at 325°C for 2 hours to pristine samples.

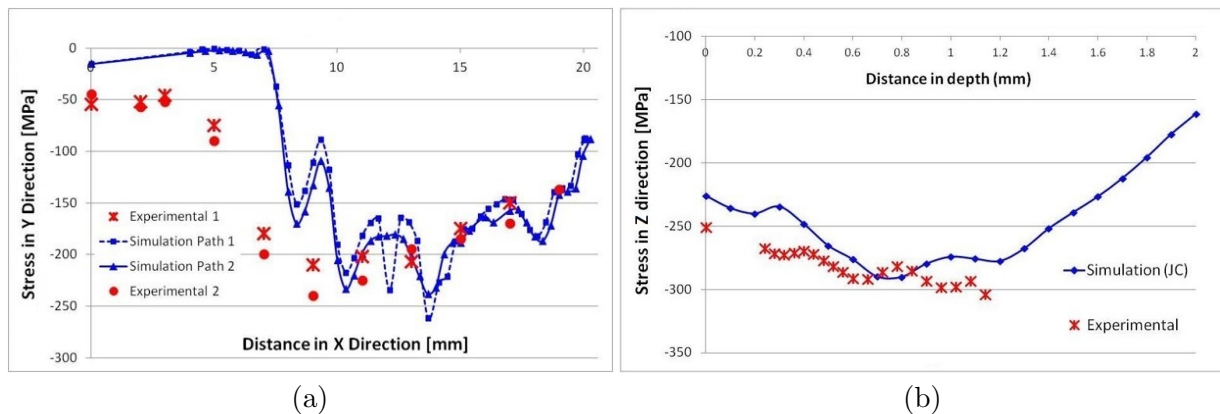


**Figure 4.** Calculated (red dots) vs measured (blue line) residual stresses: (a) stresses at the specimen surface. The measurements are taken by X-ray diffraction; (b) stresses across the specimen thickness. The leftmost experimental point (surface) was measured by X-ray diffraction, the in-depth ones by hole drilling technique.

### 3.2. Numerical simulations

Different case studies were explored in previous works to validate the numerical simulations. Troiani et al. [9] modelled a flat Al7075 specimen with a thickness of 10 mm using JC model. The residual stresses computed by the simulations were compared to experimental measurements taken by hole drilling technique and X-ray diffraction. The comparison is shown in figure 4; both surface and in-depth residual stresses are reported.

Even though the experimental techniques exhibit some scatter and exact assessment of the residual stresses is difficult, the values computed by the model are in line with the measured ones. In particular, the maximum stress (i.e. more negative) and its location are calculated quite accurately both at the surface and across the thickness.

The kinematic hardening model was used in another work [19] to model laser peening in thin aluminum panels. In particular, the work investigated the effect of laser peening on fatigue crack propagation in central-cracked panels with a thickness of 2 mm. To this end, two strips were treated with LSP at either sides of the crack. The specimen configuration and the computed residual stress distribution are shown in figure 5.

Notably, the residual stress profile in the peened strip closely resembles the one observed across the welded bead in a welded panel. The latter can be calculated using the following equation by Tada and Paris [20]:

$$\sigma(x) = \sigma_p \frac{1 - \left(\frac{x-L}{c}\right)^2}{1 + \left(\frac{x-L}{c}\right)^4}$$

where  $\sigma_p$  is the peak compressive residual stress,  $L$  is the distance between the centre of the crack and that of the peened strip and  $c$  is the point where the residual stress changes sign.

As observed in figure 5, laser shock peening in thin panel produces not only compressive stresses in the treated region, but also tensile stresses around it, which is a consequence of the global stress field being self-balanced. This effect, however, can be detrimental to fatigue crack growth, because crack propagation accelerates in the tensile region. This phenomenon was actually observed in experimental tests [19] and cautions against potential issues in using LSP as a crack stopper in thin panels. Notably, van Aswegen and Polese [21] have recently found that the sizing and placing of the peened region play a key role when improving the fatigue life of thin aluminum panels.

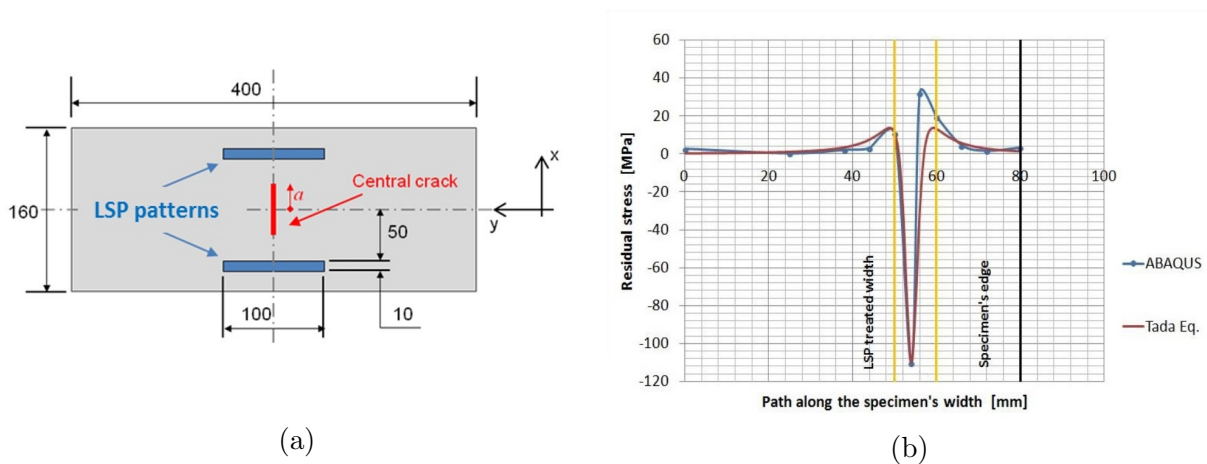


**Figure 5.** Modelling of laser shock peening in thin panels: (a) central-cracked panel treated with LSP; (b) residual stresses computed by the numerical model (in Abaqus) and those calculated using Tada's equation. The vertical yellow lines represent the edges of the peened strip.

#### 4. Conclusions

In this work, we presented the results of preliminary mechanical tests on additive-manufactured Scalmalloy specimens. In particular, the tensile strength and surface hardness of as-built and heat-treated coupons were compared. Then, we reviewed the numerical model for the computation of residual stresses in laser peened components. The main findings can be summarized as follows:

- The heat treatment seems suitable to improve the mechanical properties of the material. Both tensile strength and hardness were vastly increased in the treated samples compared to the untreated ones. Overall, the quasi-static strength of the additive-manufactured Scalmalloy is comparable to that of the aluminum alloys commonly found in aeronautical applications and produced by conventional techniques.
- Following the heat treatment, the material exhibits a more brittle behaviour, which had already been observed by other authors. Further testing is needed to clarify how this effect impacts the fatigue properties of the material.
- The numerical model is able to compute the residual stresses induced by LSP with reasonable accuracy. Different configurations can be modelled, including thick and thin panels. Specifically, in the thin panels commonly used in aeronautical structures, the distribution of tensile stresses could potentially harm the fatigue resistance. Thus, a careful choice of the peening strategy must be made to unlock the full advantages of LSP.

#### Acknowledgments

The research leading to these results has received funding from the European Union's Horizon 2020 Research and Innovation programme under Grant Agreement No 952463.

The statements made herein do not necessarily have the consent or agreement of the UMA3 Consortium and represent the opinion and findings of the authors.

#### References

- [1] Blakey-Milner B, Gradl P, Snedden G, Brooks M, Pitot J, Lopez E, Leary M, Berto F and du Plessis A 2021 *Mater. Des.* **209** 110008
- [2] Heckenberger U, Hombergsmeier E, Holzinger V and von Bestenbostel W 2011 *Proc. of the 2nd Int. Conf. on Laser Peening* (Bradford) pp 22–33



- [3] Montross C, Wei T, Ye L, Clark G and Mai Y W 2002 *Int. J. Fatigue* **24** 1021–1036
- [4] Gao Y 2011 *Mater. Sci. Eng. A* **528** 3823–3828
- [5] Ivetic G, Troiani E, Meneghin I, Molinari G, Ocaña J, Morales M, Porro J, Lanciotti A, Ristori V, Polese C and Venter A 2011 *26th ICAF Symp.* (Montreal) pp 855–866
- [6] Troiani E, Taddia S, Meneghin I and Molinari G 2014 *Adv. Mater. Res.* **996** 775–781
- [7] Glaser D, Polese C, Bedekar R, Plaisier J, Pityana S, Masina B, Mathebula T and Troiani E 2014 *Adv. Mater. Res.* **891-892** 974–979
- [8] W B and R B 1999 *Int. J. Fatigue* **21** 719–724
- [9] Troiani E, Crudo C, Molinari G and Taddia S 2013 *27th ICAF Symp.* (Jerusalem) pp 5–7
- [10] Taddia S and Troiani E 2015 *Mater. Today Proc.* **2** 5006–5014
- [11] Troiani E and Zavatta N 2019 *Metals* **9** 728
- [12] Peyre P, Sollier A, Chaieb I, Berthe L, Bartnicki E, Braham C and Fabbro R 2003 *Eur. Phys. J. Appl. Phys.* **23** 83–88
- [13] Johnson G R and Cook W H 1983 *Proc. 7th Int. Symp. on Ballistics* (The Hague) pp 541–547
- [14] Chaboche J 1986 *Int. J. Plast.* **2** 149–188
- [15] Chen Y, Clausen A, Hopperstad O and Langseth M 2009 *Int. J. Solids Struct.* **46** 3825–3835
- [16] Raab M and Bambach M 2023 *J. Mater. Process. Technol.* **311** 117811
- [17] Spierings A, Dawson K, Kern K, Palm F and Wegener K 2017 *Mater. Sci. Eng. A* **701** 264–273
- [18] Ren Y, Dong P, Zeng Y, Yang T, Huang H and Chen J 2022 *Appl. Surf. Sci.* **574** 151471
- [19] Troiani E, Taddia S, Meneghin I, Molinari G and Polese C 2015 *28th ICAF Symp.* vol 1 (Helsinki) pp 466–476
- [20] Tada H and Paris P C 1983 *Int. J. Fract.* **21** 279–284
- [21] van Aswegen D and Polese C 2021 *Int. J. Fatigue* **142** 105969